Integrated Modeling and Optimization of Lunar In-Situ Resource Utilization Systems

Samuel S. Schreiner
Massachusetts Institute of Technology
Cambridge, MA 02139
sschrein@mit.edu

Jeffrey A. Hoffman
Massachusetts Institute of Technology
Cambridge, MA 02139

Gerald B. Sanders
Johnson Space Center
Houston, TX 77058

Kristopher A. Lee
Johnson Space Center
Houston, TX 77058

***Abstract*—The production of oxygen from lunar regolith, a form of In-Situ Resource Utilization (ISRU), is a mission-enabling technology that can break the supply logistics chain from Earth to support sustained, affordable space exploration. We present the development of an integrated ISRU system model to study and optimize the system mass and power requirements, a critical development in understanding the proper application of ISRU systems. The integrated model includes subsystem models for a Molten Regolith Electrolysis (MRE) reactor, an excavator, a hopper and feed system, the power system, and an oxygen liquefaction and storage system. A hybrid genetic-algorithm/gradient-based optimization scheme is implemented to optimize the ISRU system design across a range of production levels. Lower oxygen production levels (<1500 kg/yr) are best managed with a single reactor operating at a traditional temperature of 1900K and a batch time of 2-3 hrs. Larger oxygen production levels are best met with multiple reactors that each produce ∼2500 kg/yr, operate at 2200K, and have a batch time around 1 hr. It is found that an MRE reactor can generate the entire ISRU system's mass worth of oxygen in as little as 52 days at a rate of 7 kg of oxygen annually per kilogram system mass.**

TABLE OF CONTENTS

1. INTRODUCTION

One of the most significant barriers to space exploration is the burden of bringing all of the material resources from Earth required for a mission. To enable sustainable, affordable space exploration, the reliance on Earth's resources must be reduced. In-situ resource utilization (ISRU), or leveraging extraterrestrial resources to support space missions, can significantly reduce the required launch mass and cost for a given mission [1, 2].

One avenue for utilizing space resources is producing oxygen on the lunar surface. The production of oxygen from lunar regolith is a architecture-enabling technology that can significantly reduce the supply logistics chain from Earth. Oxygen is a major component of launch vehicle, spacecraft, and lander masses (∼70% of launch vehicle mass) and at the same time is one of the most abundant lunar resources (lunar soil is ∼44% oxygen by weight) [3]. The production of this valuable resource outside of Earth's gravity well can support lunar surface activities or enable orbital refueling to drastically reduce mission cost. The 1993 "LUNOX" study by Johnson Space Center investigated the possible benefits of producing oxygen on the Moon for early lunar exploration missions and found an associated reduction in launch vehicle mass and a 50% reduction program cost.

Sherwood and Woodcock [2] conducted an economic analysis of producing oxygen on the lunar surface to supply lander ascent propellant. They determined that lunar ISRU has great potential to be economically feasible, but *"the sensitivities* [of their economic model] *are modest, except for the mass of production hardware*" [2]. Thus, it is imperative to accurately model the mass and performance of ISRU systems to determine economic feasibility. Furthermore, ISRU system models can provide guidance for both the hardware development and mission applications of such systems [4].

The oxygen in lunar soil is primarily bound up in oxides and there are over twenty different oxygen extraction methods proposed in the literature [1, 5, 6]. In the past decade, three of these methods have undergone dramatic technology maturation: Hydrogen Reduction of Ilmenite (HRI), Carbothermal Reduction of Silicates (CRS), and Molten Regolith Electrolysis (MRE) [7]. Previous research has extensively modeled HRI and CRS reactors [4, 8, 9, 10, 11] but a suitably mature model for an MRE reactor has only recently been developed [12]. MRE is an electrochemical processing technique that performs direct electrolysis on molten lunar regolith to produce gaseous oxygen at the anode and liquid metals at the cathode.

There is a strong impetus to explore the feasibility of an ISRU system with an MRE reactor, as there are many potential benefits to such a system. Utilizing MRE may result in considerable mass savings compared to the other two primary techniques (HRI and CRS), as it can theoretically extract all of the oxygen from lunar regolith [13]. MRE does not require either a gas recycling system or a water electrolyzer, which may also reduce system mass. Other benefits include the synergistic production of materials such as iron, silicon, aluminum and glassy materials. These byproducts of oxygen production can be used to construct spare parts, buildings and solar arrays on the lunar surface [14]. Conversely, MRE may require more power due to the high operating temperature compared to HRI or CRS. Additionally, MRE is at a lower technology readiness level (TRL) and thus requires more technology development.

In light of the recent evidence in support of water in the polar lunar craters [15], there remain many potential benefits to using MRE on the lunar surface, perhaps even in parallel with a water extraction scheme. First, there is significant

978-1-4799-5380-6/15/$31.00

uncertainty as to the state and concentration of the water in lunar craters [15]. A resource prospecting mission is necessary to ascertain ground truth and is currently planned to launch in 2019 [16]. MRE may be concurrently developed using composition data from the Apollo lunar samples. Technical challenges associated with feedstock excavation on the poles, especially excavation from within permanently shadowed craters, can also be avoided with the MRE process.

This work integrates an MRE reactor model [12] into an ISRU system model. Previous work in integrated ISRU system modeling provided a foundation for this analysis, but did not include a power system, and suitable models for an MRE reactor and excavation system were not available at the time [9, 17]. The system model presented in this work expands upon previous work to encapsulate a more complete system by including subsystem models of the reactor, power system, excavation system, oxygen storage and liquefaction system, as well as a hopper and regolith feed system. By evaluating the integrated ISRU system, the holistic system performance may be studied and optimized, rather than just the reactor subsystem. A hybrid genetic algorithm/gradient-based optimization routine is developed, validated, and exercised to minimize the ISRU system mass over a range of oxygen production levels.

Section 2 provides an overview of the subsystem models. In Section 3, the integrated system model is presented and the details of the subsystem connections are presented with an N^2 diagram. Section 4 provides an overview of the optimization technique implemented on the ISRU system model. In Section 5, the optimized system design over a range of oxygen production levels is explored. Section 6 concludes with some key aspects of the optimized system and provides recommendations for future work.

2. System Model Description

Reactor

Although a variety of reactor models can be integrated into the system model, this work utilized a Molten Regolith Electrolysis (MRE) reactor model [12] to better understand the system-level implications of that processing technique. As shown in Figure 1, the reactor modeled includes an outer cylindrical shell with three layers: an outer structural layer, a middle insulation layer, and an inner refractory layer for managing the corrosive molten metals produced. The anode and cathode, composed of a shaft and plate, extend into the molten region from the top and bottom, respectively. The red lines depict current streamlines through the inner molten core of the reactor.

The reactor model uses electrochemistry to estimate the current and voltage. The current is directly related to the oxygen production rate:

$$I = (\dot{n}_{O_2})\frac{nF}{\bar{\eta}}, \tag{1}$$

where $\dot{n}_{O_2}$ is the desired molar oxygen production rate (mol/s), n is the number of electrons required per diatomic oxygen (4), F is Faraday's constant, and $\bar{\eta}$ is the average current efficiency over an entire batch. The instantaneous current efficiency depends upon which oxide is currently being electrolyzed and can range from 30-60% for iron oxides and is near 100% for melts once the iron oxide has been depleted [18]. This means that the average efficiency depends upon the composition of regolith and will therefore

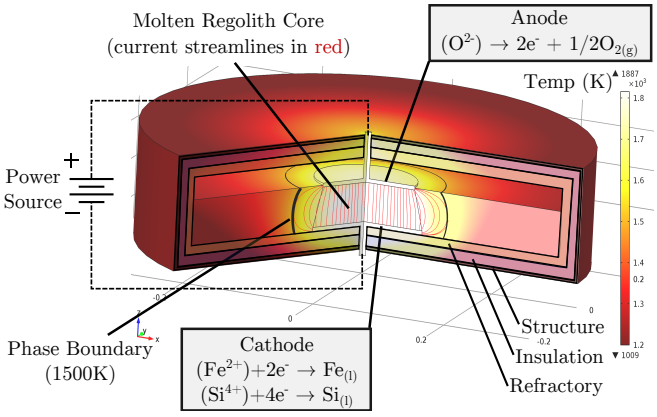

Figure 1. The anatomy of a Molten Regolith Electrolysis (MRE) reactor. Also shown are the temperature and current profiles from a multiphysics simulation that was used to predict reactor performance and tune reactor design.

be dependent upon lunar location. For example, the higher iron concentration in the mare regions will result in a lower average current efficiency [12].

The reactor model translates the oxygen production rate into the required regolith processing rate using the fraction of oxygen that can be extracted from regolith. Due to the fact that an MRE reactor can extract oxygen from all oxide species in lunar regolith, the contribution from each oxide specie must be summed together:

$$\frac{m_{oxygen}}{m_{regolith}} = \sum_i (w_i)\frac{MW_{O2}}{MW_{oxide,i}}(r_{mol,i})(e_{frac,i}) \tag{2}$$

where w_i is the weight percent of oxide i in lunar regolith, MW is the molar weight (of oxygen or an oxide), $r_{mol,i}$ is the number of moles of oxygen per mole of oxide i ($\frac{mol_{O2}}{mol_{oxide}}$), and $e_{frac,i}$ is the fraction of oxide i that is electrolyzed in each batch. The fraction of each oxide specie that can be electrolyzed is strongly dependent upon operating temperature, because the solidification temperature of the melt generally increases throughout electrolysis. In the MRE reactor model, the electrolysis process is allowed to progress until the melt solidification temperature is within 50 K of the operating temperature to allow for a safety margin. Thus, higher operating temperatures allow the reactor to extract more oxygen per kilogram regolith, but also results in a higher heat loss to the environment. This is one tradeoff that is optimized using the system model.

One key factor in the design of an MRE reactor is the containment of molten regolith. Molten lunar regolith is extremely corrosive and cannot be contained for extended periods of time by traditional crucible materials [13]. A joule-heated, cold-wall reactor, similar to the Hall-Heroult cells in the aluminum production industry, is an elegant solution to the challenge of molten regolith containment. In this concept, the reactor maintains a molten regolith core via the heat generated by the current passing through the resistive melt, while the molten region is surrounded by solid regolith that insulates and protects the side walls of the reactor from corrosion [19].

To facilitate this complex electrothermodynamic process, the diameter, electrode separation, and thermal characteristics of the reactor must be carefully designed. To address this design challenge, a multiphysics simulation of an MRE reactor was utilized to create a tradespace of over 40,000 unique reactor designs. Multivariate nonlinear regression equations were fit to this tradespace to create a parametric sizing model for an MRE reactor. The regression equations are used to tune the reactor diameter, electrode separation, and reactor wall thermal conductivity to meet the required average current from Equation 1, the molten mass from Equation 2, and the operating temperature (set as a reactor model input), while also ensuring that no molten material touches the reactor wall [12]. Figure 2 shows the behavior of these three design variables over a range of oxygen production levels for two different operating temperatures, as detailed in [12]. Figure 1 shows one feasible design generated using this novel design methodology.

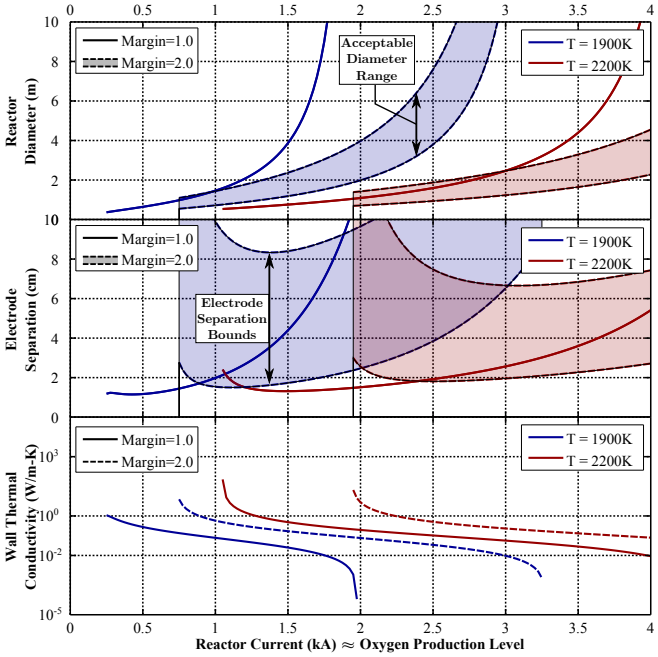

Figure 2. The required reactor diameter, electrode separation, and wall thermal conductivity (bottom) plotted over a range of reactor currents. *Note: The molten mass in the reactor is also scaled up with current to make the x-axis a surrogate for oxygen production level.*

As detailed in [12], the reactor design methodology includes a design variable called the *"design margin"*, which describes the flexibility in the reactor design. There is a maximum reactor diameter that satisfies the operating temperature and a minimum diameter that satisfies the required mass of molten regolith in the reactor. These two bounds on reactor diameter can be varied by changing wall thermal conductivity, and the design margin describes the ratio of these two diameter bounds. A design margin of 1.0 results in the minimum and maximum diameter bounds being equal, while a margin of 2.0 results in a maximum diameter bound that is twice the minimum. Having a range of acceptable reactor diameters results in an acceptable range of electrode separations, which enables a variable electrode separation during operation to control operating voltage and heat production. Design margin can be considered as a surrogate for traversing the design space between the optimality and flexibility of an MRE reactor design. The plots in Figure 2 show how varying the design margin affects the required diameter, electrode separation, and wall thermal conductivity.

In this work, the primary reactor design variables that are optimized include the number of reactors, operating temperature and design margin. Future work can address optimizing additional parameters, but these three variables were chosen because they are the primary drivers of MRE reactor design.

YSZ Separator

A Yttria-Stabilized Zirconia separator is included in the system model to separate oxygen from the MRE reactor exhaust gas. Although the molten electrolysis process produces pure oxygen by electrolyzing oxides into oxygen gas and liquid metals, certain species (Na_2O, P_2O_5, K_2O and MgO) will evaporate after electrolysis and will likely become entrained in the oxygen flow as contaminants. Additionally, trace gases such as H_2, N_2, CO_2, and Helium will also be released as fresh regolith is heated up to a molten state [20].

Yttria-Stabilized Zirconia (YSZ) is a ceramic material composed of zirconimum dioxide (ZrO_2) stabilized by the addition of yttrium oxide (Y_2O_3). YSZ is commonly used as an electroceramic to measure oxygen content by monitoring the voltage across conductive platings on each side of the solid YSZ electrolyte. As shown in Figure 3, to act as a separator, an active voltage is applied across the electrodes while the gas flow encounters the cathode. At the cathode, oxygen gas (O_2) is ionized to O^{2-} and then transported through the YSZ electrolyte via the electric field between the plates.

The power demand of the separator is estimated by determining the required current and voltage. The current is directly proportional to the amount of oxygen that needs to be transported through the separator and was calculated using Equation 1 with a current efficiency of one (assuming no other species are transported through the separator). To estimate the voltage, the electrical conductivity of YSZ needed to be modeled. Data on the temperature-dependent conductivity (σ) of YSZ [21] was fit with the equation:

$$ln(\sigma(T)) = a * exp(b * T) \ \ [S/cm] \tag{3}$$

where the fit coefficients are $a = -23.4 \pm 4.8$ and $b = -0.00259 \pm 0.0003$ and the temperature, T, is in Kelvin. The temperature dependence in the YSZ conductivity couples the separator model and the reactor model: a higher operating temperature in the reactor results in a higher electrical conductivity of the YSZ separator which decreases the power required for the separator. For simplicity, temperature of the YSZ was taken to be 75% of the reactor operating temperature. This was intended as a preliminary estimate to couple reactor temperature and YSZ temperature, while also accounting for some heat loss between the reactor and separator. Future work can generate a more accurate model of the expected temperature at the separator as a function of reactor temperature. The electrical conductivity was then used to calculate the resistance of the YSZ separator (R_{YSZ}):

$$R_{YSZ} = \frac{\Delta x}{\sigma(T)\, S}, \tag{4}$$

where Δx is the thickness of the YSZ separator (assumed to be 0.5 cm), $\sigma(T)$ is the YSZ electrical conductivity calculated from Equation 3, and S is the required cross-sectional area of

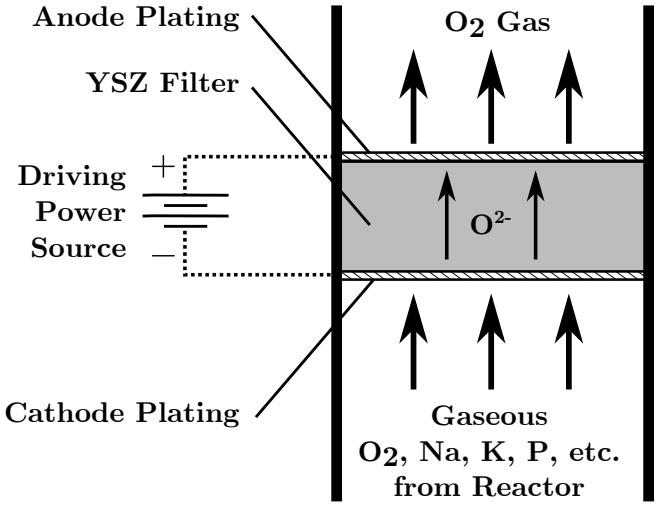

Figure 3. A diagram of the proposed YSZ schematic for use with the Molten Regolith Electrolysis reactor.

the YSZ separator calculated as:

$$S = \frac{I_{YSZ}}{j}, \tag{5}$$

where I_{YSZ} is the required current through the YSZ separator and j, the limiting current density, was taken to be 0.4 A/cm^2 [22]. The power of the YSZ ceramic was estimated using the current and resistance (I^2R). The dimensions of the separator and a 304 Stainless Steel casing are used to calculate the YSZ separator mass.

It should be noted that the YSZ separator model is a simplified version with the intention of determining the power needed for oxygen separation with only first-order estimates of mass and volume. It is believed that the power requirement of the YSZ separator will play a much more significant role than its mass in the ISRU system optimization. YSZ oxygen separators are commonly composed of multiple packed tubes or stacked wafers, which could reduce the mass and volume estimates, but not significantly change the power requirement, compared to this simplified YSZ model. A more realistic mass model will be created in a future iteration.

Excavator

The excavator system, developed at the Glenn Research Center [23], predicts the mass of a mobile excavation platform sized to deliver the regolith throughput requirement to the reactor. A force module utilizes the Balovnev force equations to generate estimates of the force and torque involved in excavating lunar regolith. A hole depth of 25 cm with cut depths of 2.5 cm was used to size a front-end loader in this system model. The excavation force estimates are used to size the excavation actuators using commercial off-the-shelf (COTS) actuators and controllers from Danaher[2]. The force module also determines the vehicle reaction and traction forces. A mass module conducts a structural analysis to ensure that the excavator chassis can support the regolith weight and that the digging mechanism can support the expected excavation stresses. The locomotion motors are modeled after the Maxon motors used on the Mars Exploration Rover [24].

An excavator speed of 0.5 m/s and a plant distance of 100 m are used to properly size themobility platform for the excavator. Information on the excavator operating duty cycle based on the power system charge/recharge cycle is also incorporated into the model. The excavator model utilizes all of this information to generate an excavator design that can meet the regolith delivery requirements from the reactor while withstanding the excavation forces and regolith load requirements.

Hopper and Feed System

The main driver in the hopper model is the buffer capacity, or the amount of regolith the hopper had to hold in terms of days of reactor operation. A buffer capacity of 2 days was chosen to ensure that the hopper could hold enough regolith for continual reactor operation if the excavator needed repairs. Furthermore, a buffer capacity of 2 days effectively decouples the excavation system scheduling from reactor batch mode operation (i.e. although the reactor may operate on a 1 hour batch time, the excavator can deliver regolith with a lower frequency).

The feed system model calculates the mass and power of the system required to insert fresh regolith from the hopper into the reactor. An auger was chosen for this design iteration, but other methods, such as a pneumatic feed system, can be modeled in the future. The feed system model sizes an auger that extends from the reactor through a cylindrical sleeve and into the hopper. Using estimates of the cohesion, internal and external friction angles, and soil-tool adhesion values for lunar regolith, the feed system model estimates the expected torque on the auger and the resultant power consumption. The number of feed systems is set equal to the number of reactors, as each reactor will likely require its own feed system. The sleeve and auger are made out of Hastelloy C-276, due to the interface with the high-temperature reactor.

One assumption built into the feed system model is that a 5 cm diameter auger rotating at 5 rpm would be adequate to insert a full batch of regolith in the feed time set as an input in the reactor model. That is, for larger amounts of regolith per batch, the feed system was not parametrically sized up, due to limitations in the model design. Future work can expand the feed system model to dynamically size the radius and rotational rate of the auger system to meet the required regolith mass flowrate.

Oxygen Liquefaction and Storage

The oxygen liquefaction and storage system utilizes oxygen production data from the reactor to size both the liquefaction and storage systems. The liquefaction system determines the mass and power of the system required to liquefy the oxygen coming from the reactor, as well as the cooling power required to re-liquefy oxygen that has boiled off in the storage system.

For the storage system, a capacity of 6 months was chosen to allow for sufficient propellant production to support two refueling missions per year. The number of layers of MLI can be chosen to balance heat loss with system mass. Based off of a user material selection, the storage system is sized such that the yield stress is less than the hoop stress with a factor of safety of 2. The tank size and number of layers of MLI directly impact the boiloff rate due to expected heat leakage into the tank.

[2]http://www.danahermotion.com

Power System

The power subsystem is parametrically sized from the total power requirement summed over all of the other subsystems, as shown in Figure 4. A number of options are available in the power model, including solar arrays without energy storage (day-only operation), solar arrays with fuel-cell energy storage to enable lunar night operation, a Stirling radioisotope generator, and a fission surface power system. To reduce the design tradespace, this study restricted the power system to be solar cells that provide power to the ISRU system for day-only operation. From a prior NASA study, using this type of power system in the Shackleton crater rim area resulted in an approximate duty cycle of at least 0.7 (>70% of the year with continuous uninterrupted solar power), due to the longer day duration near the lunar poles. Other locations have a corresponding duty cycle of 0.5. The specific mass of the solar array power system without energy storage was taken to be 20 kg/kWe [25]. Future work can evaluate the effectiveness of other power systems in the context of a lunar ISRU system.

3. ISRU System Integration

The subsystem models described in the preceding section are integrated together into a holistic system model. By linking the subsystems (reactor, excavator, power, etc.) together into a self-consistent model, the entire mass and power of an ISRU system can be estimated. The self-consistency of the model allows the tradeoffs between subsystem designs to be studied. For instance, shortening the batch time of an MRE reactor is one avenue for reducing reactor mass. But this reduction in reactor mass comes at the cost of an increase in reactor power due to the increase in total down time between batches which reduces total operational time. The integrated model enables a more complete study of the optimal batch time, as one example, by including the mass of both the power and reactor subsystems.

Another important design variable to optimize is the reactor operating temperature. Higher operating temperatures intuitively result in more radiative heat loss and increase the heating power per kilogram regolith. Conversely, higher temperatures decrease the regolith throughput requirement by increasing the amount of oxygen extracted per kilogram regolith. From an electrochemical point of view, higher temperatures result in a more endothermic reaction. The integrated ISRU system model provides a framework to study the optimal operating temperature.

Figure 4 depicts an N^2 diagram of the ISRU system. The primary subsystem couplings are shown, with some secondary connections left out for clarity. It is evident that the reactor, described in detail in [12], is a strong driver of many other system designs, as one would expect. It is a large driver of the power requirement and also sets the regolith processing requirement which directly affects the excavator, hopper and feed systems. The power requirement from each subsystem is summed together and used to size the power system. After the power system is sized, the mass of all of the subsystems, including the power system, are summed together to generate an estimate of the total ISRU system mass.

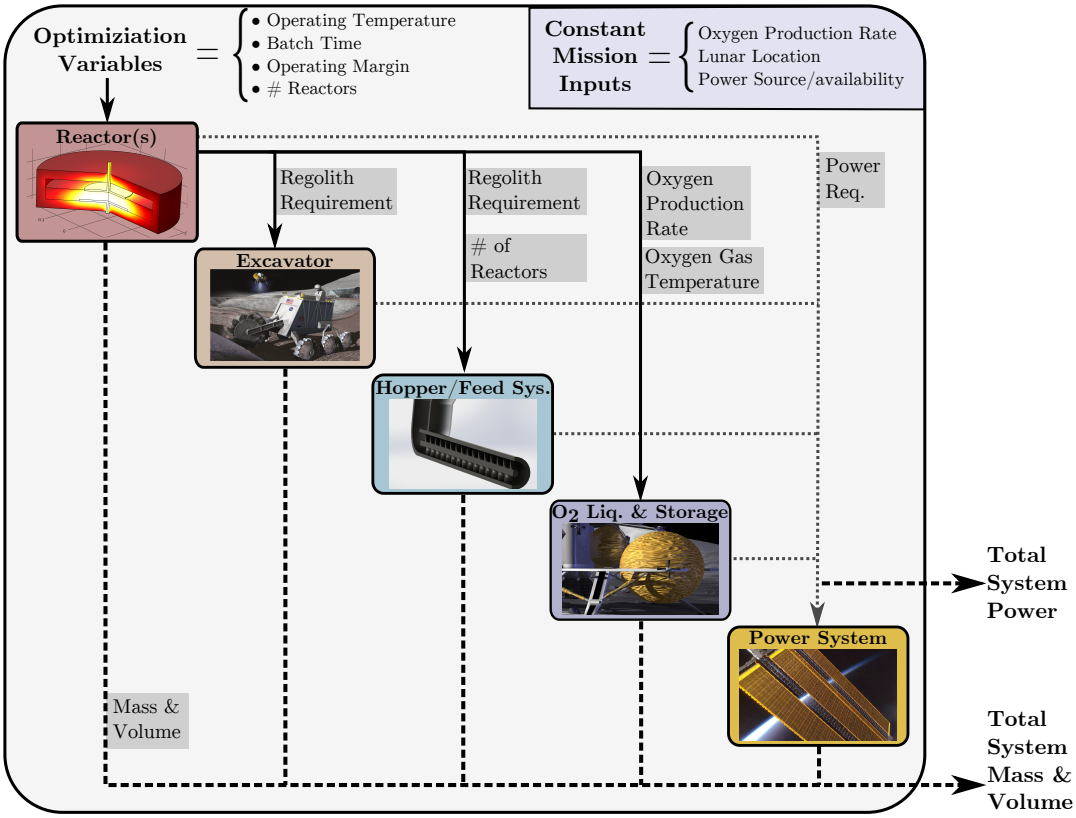

Figure 4. An N^2 diagram of the ISRU system model within the optimization routine, showing how the subsystems are interconnected to generate a self-consistent estimate of system mass, which is then optimized.

4. OPTIMIZATION TECHNIQUE

A genetic algorithm (GA) optimization routine was used with the holistic system model to optimize the ISRU system design by varying subsystem design variables. A genetic algorithm method was implemented, rather than traditional gradient-based optimization techniques, due to the mixed-integer nature of the system: although some parameters were continuous, such as operating temperature, the majority of parameters were discrete, such as number of reactors or excavators and material selections. A genetic algorithm is a heuristic search method that attempts to mimic natural selection by generating a population of candidate designs in what is called a generation. The fitness (or goodness) of each generation is evaluated and the characteristics of the top-performing candidates are recombined/mutated to form the subsequent generation. The genetic solver terminates when the fitness function does not significantly change over a number of generations.

A sample output from the genetic algorithm solver is shown in Figure 5. The "Mean penalty value" markers depict the mean system mass within the entire population of systems designs in a given generation. The "Best penalty value" shows the lowest mass ISRU system in a given generation.

Although GA is a suitable technique for optimization over discrete variables, it is not particularly well suited to optimized a large number of continuous parameters. To enable a more efficient optimization, a gradient-based optimizer was implemented that used the final GA solution as a starting point with the integer variables fixed. The ISRU system model is nonlinear and contains no analytical gradient, so the solver used finite difference approximations for the gradient. In this manner, the GA optimizer was used to find the general global minimum region while avoiding local minimums, and the gradient-based optimizer was used to hone in on the true minimum.

Many of the subsystem models contained error flags that identified infeasible reactor designs, vehicle slippage, and a number of other system model errors. A set of soft constraints were implemented by penalizing the mass of systems with error flags by a factor of 5. In this manner the hybrid optimization scheme selectively removed system designs with error flags due to the system mass penalty.

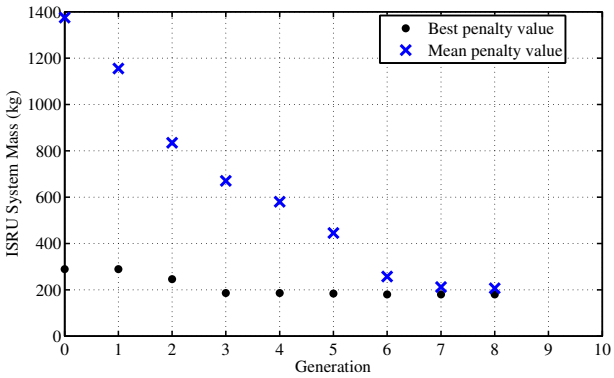

Figure 5. A sample output from the genetic algorithm optimizer used on the ISRU system model, where the penalty value is the mass of the ISRU system (kg). The downwards trend in the blue data shows the effectiveness of the "natural selection" of better performing candidates from generation to generation.

5. ISRU SYSTEM OPTIMIZATION

Tradespace Optimization

This study looked at optimizing the batch time, number of reactors, MRE reactor operating temperature, and MRE design margin (described in Section 2) to minimize the integrated ISRU system mass. Figure 6 shows the the growth of the ISRU system mass and power over a range of oxygen production levels in the top two plots. The remaining graphs (with labels) depict the optimized system design tradespace, including the number of reactors (a), operating temperature (b), reactor diameter (c), molten mass per batch (d), average reactor current (e), operating voltage (f), batch time (g) and the MRE design margin (h). It should be emphasized that the operating current and molten mass per batch are both for a single reactor, not for the combined reactors when multiple are present.

The top left plot in Figure 6 examines the growth in the ISRU system mass breakdown over a range of oxygen production levels. The most significant mass drivers are the oxygen liquefaction/storage system and power system, which comprise 26% and 54% of the system mass at a production level of 10,000 kg/yr, respectively. As mentioned in the model description, the oxygen storage system was designed to hold 6 months of oxygen production at any given time, and this requirement may be relaxed depending upon the mission needs. The reactor and YSZ separator compose approximately 6% of the entire ISRU system mass at an oxygen production level of 10,000 kg/year. The total system mass curve was fit with the following power-law curve:

$$M = 0.52 * N^{0.86}, \tag{6}$$

where M is the ISRU system mass and N is the annual oxygen production level. The fact that the power coefficient is less than one implies that the ISRU system exhibits an economy of scale. That is, the ISRU system produces higher quantities of oxygen more efficiently.

A number of interesting trends exist in the optimized system parameters shown in the lower plots of Figure 6. The optimal number of reactors (Plot *a* in Figure 6) behaves as one would expect. At low production levels a single reactor is preferable, but as production level increases, more reactors are selected to meet the production demand. This indicates that there is an maximum optimal oxygen production for a single reactor. That is, for MRE, there is an optimal reactor design for somewhere near 2500 kg/yr and increasing oxygen production rate significantly beyond this threshold can best be met by increasing the number of reactors rather than by tuning reactor design.

The optimal operating temperature (Plot *b* in Figure 6) also displays some interesting behavior. In the optimization routine, operating temperature was given hard bounds between 1873 k and 2200 K (illustrated by the black dotted lines). Below 1873 K, the reactor comes dangerous close to the solidification temperature of iron and runs the risk of producing solid iron and "freezing" the reactor. Above 2200 K, the MRE model was not sufficiently tested to produce reliable results. The optimal operating temperature begins around 1900 K at 500 kg/yr, and rises to the 2200 K ceiling

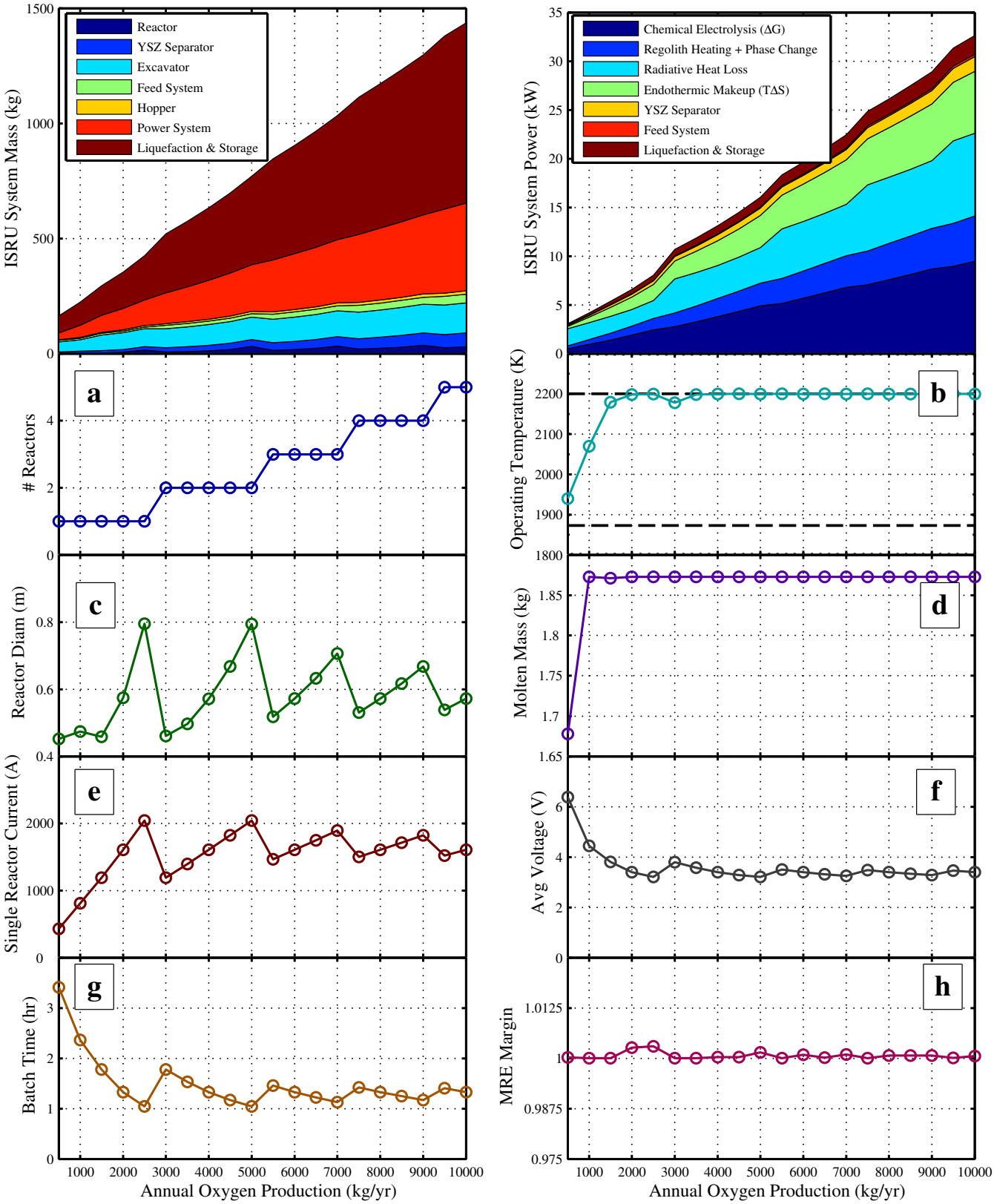

Figure 6. (Top) The system mass and power breakdowns over a range of oxygen production levels. The optimized variables in the system design, with an emphasis on the reactor design that results from the optimized holistic ISRU system.

for higher production levels. A small decrease in operating temperature occurs when the second reactor is added to the system to meet the production level of 3000 kg/year. The rise to higher temperatures is likely due to the fact that electrolyzing at higher temperatures allows more oxygen to be extracted per kilogram regolith, which reduces regolith throughput requirements and reactor size [12]. Prior to this analysis, it was unclear whether or not these benefits would be outweighed by the increased heat loss, increased regolith heating requirement (per kilogram regolith), and resultant power system increase. The integrated system model showed that operating temperatures higher than the traditional 1873 K do indeed result in a lower total system mass at high production levels.

The reactor diameter (*plot c*) appears to grow with oxygen production level, and then decreases each time the number of reactors increases. This shows that at certain oxygen production levels, in order to increase production it is optimal to incorporate an additional reactor rather than increase reactor size. The reactor diameter appears to have a minimum of approximately 0.45 m and does not grow larger than 0.8 m for the oxygen production levels studied in this work ($<$10,000 kg/yr).

The molten mass per batch (*plot d*) appears to have an optimal value of around 1.87 kg/batch. Deviations from the optimal value occur only at low production levels. Future work will have to further analyze the source of this optimal value.

The current per reactor (*plot e*) intuitively increases with oxygen production level, and then decreases each time the number of reactors increases. It would appear that a maximum current of around 2000 A per reactor is optimal. Above this limit the reactor must grow exponentially to accommodate the additional heat load. Note that the current line is roughly linear with a slope that is inversely proportional to the number of reactors. Deviations from linearity occur due to the change in current efficiency with operating temperature, as detailed in [12].

The average reactor voltage (*plot f*) decreases asymptotically from a value of approximately 6 volts at a production level of 500 kg/yr to around 3.25 volts at higher production levels. This is a result of increased current per reactor as shown in plot *e*. As the current in each reactor increases, the voltage can decrease while still generating enough heat to maintain the molten core. Each time a reactor is added to the system, we observe a slight increase in voltage which then returns towards the asymptote.

The optimal batch time (*plot g*) appears to decrease in a piecewise asymptotic manner from approximately 3.5 hours at a production level of 500 kg/yr to slightly more than 1 hour at higher production levels. A small increase in batch time occurs when the number of reactors increases.

The MRE reactor design margin (*plot h* in Figure 6) also exhibits interesting behavior. It stays reasonably close to 1.0 across all oxygen production levels, with the most significant deviation of less than 1.01 occurring at 2500 kg/yr. A margin of close to 1.0 is certainly intuitive, as the margin describes the tradeoff between minimal power consumption (margin=1) and increased reactor design flexibility (margin$>$1). Although margin was bounded between 1.0 and 10.0 in the optimization, the GA-optimizer would often select optimal margin values between 1.0 and 2.0 and the gradient-optimizer would then find optimal values within 1% of 1.0. It is worth noting that margin increases away from 1.0 prior to the addition of another reactor to the system, indicating that the reactor design is being stretched away from the optimal reactor production level. The MRE margin always returns to a value of 1.0 at higher production levels with the addition of another reactor.

The top right plot in Figure 6 examines the the growth in the ISRU system power breakdown in more detail. The "Chemical Electrolysis (ΔG)" section represents the power required to break the chemical bonds in the oxides in lunar regolith. The "Regolith Heating + Phase Change" section represents the power required to heat the regolith up from the ambient temperature of $\sim$400K to the operating temperature ($\sim$2000K), including the latent heat of melting in the phase change. "Radiative Heat Loss" is predicted by the regression equations discussed in Section 2. The "Endothermic Makeup" slice depicts the amount of power required to maintain thermal equilibrium throughout the endothermic electrolysis reaction. "YSZ Separator", "Feed System", and "Liquefaction and Storage" power demands are discussed in Section 2.

Optimization Method Comparison

Figure 7 shows the mass the ISRU system optimized by the genetic-algorithm (GA) routine and by the hybrid method described in Section 4. As one would expect, the hybrid method results in system masses that are the same or lower compared to those found using the GA routine. On average, the ISRU system mass from the hybrid optimizer was 11.4 kg less than the GA method alone. The maximum mass difference between the two optimized systems was 45.9 kg. Although not shown, similar trends were observed in the ISRU system power. The hybrid-optimized system had a power consumption of 0.29 kW less, on average. The largest difference observed was when the hybrid optimized system had a power consumption of 1.0 kW less than the system generated by the GA optimization alone.

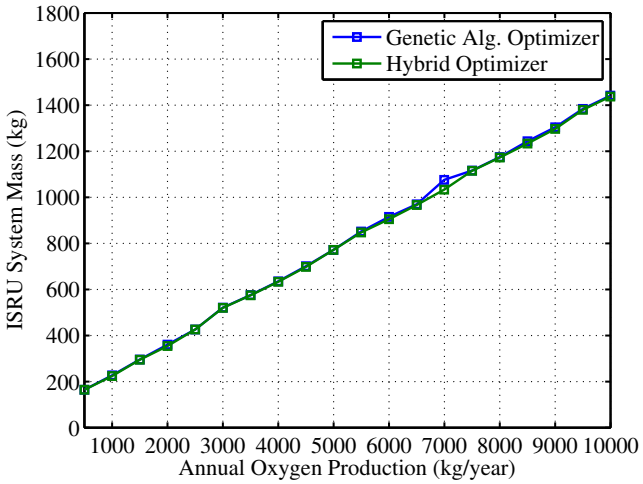

Figure 7. The mass of the optimized ISRU system across a range of production levels. The system designs generated by the hybrid optimization scheme are compared to those generated by the genetic algorithm alone.

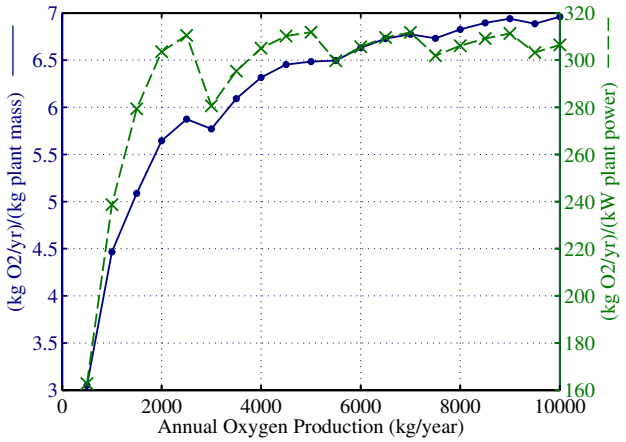

Figure 8. The oxygen production level normalized by holistic ISRU system mass (blue) and holistic ISRU system power (green).

ISRU System Utility

With any ISRU system, it is important to compare the utility of the system to a baseline concept of simply bringing along the resources from Earth. Figure 8 shows the annual oxygen production normalized by the mass (blue) and power (green) of the complete ISRU plant, which are measures of the plant efficiency. It is clear that at higher production levels an MRE-based ISRU system is able to produce more oxygen per unit plant mass and power. The oxygen production level normalized by system mass increases with production level, indicating that the ISRU system utilizing an MRE reactor can meet higher production levels more efficiently. Within the production levels studied in this work, the maximum efficiency of ∼7 kg oxygen per kilogram ISRU system mass was observed at the maximum production level of 10,000 kg/year.

To further understand the utility of an ISRU system, the number of days until the plant produces its mass in oxygen was also calculated. Using the data in Figure 8, it was determined that at an oxygen production level of 10,000 kg/year, it takes around 52 days for the ISRU system to "pay off" and produce its mass in oxygen. At a production level of 500 kg/yr, it will take 120 days to "pay off". It should be noted that this analysis does not include economic considerations, future work will investigate the price of oxygen produced and the cost of developing and emplacing the ISRU system. For this analysis, examining the mass "pay off" point provides a first-order surrogate for determining the tipping point in system utility.

6. CONCLUSIONS

Optimal System Design

This paper presents estimates of the mass and power of an optimized ISRU system to extract oxygen from lunar regolith. To accomplish this, a Molten Regolith Electrolysis reactor model is integrated with models for a power system, excavator, hopper, regolith feed system, and oxygen liquefaction and storage systems. This integrated model is leveraged in a hybrid genetic-algorithm/gradient-based optimization scheme to generate optimized system performance and design estimates across a range of oxygen production levels.

The trends in the ISRU system mass (shown in Figure 6) exhibited an economy of scale, indicating that higher production levels can be met more efficiently. At a production level of 10,000 kg/year, the ISRU system can produce 7 kg of oxygen annually per kilogram system mass. This translates to the ISRU system being able to produce the entire system mass in oxygen in 52 days at a production level of 10,000 kg/year. At low production levels (∼500 kg/yr), it would take approximately 120 days. If the Molten Regolith Electrolysis process is also leveraged to produce molten metals for manufacturing, the number of days till mass payoff would be significantly reduced.

The power system plays the largest role in system mass, comprising 54% of the holistic system mass. The power system mass could be reduced by better limiting heat loss from the reactor, which is a primary driver of total system power. Although MRE reactors need to lose a certain amount of heat through the side walls to enable a molten core surrounded by solid regolith, the top and bottom of the reactor could possibly be better insulated to reduce heat loss.

The oxygen liquefaction and storage system was also a major mass driver, comprising 26% of the holistic system mass. The system was sized to hold 6 months of oxygen production, which results in significant amount of stored oxygen at higher production levels. The 6 month storage requirement may not be necessary at higher production levels, as oxygen may also be used more frequently.

The optimization confirmed that an MRE reactor design margin close to 1.0 is indeed optimal for minimizing the combination of reactor mass and power system mass. This was previously somewhat uncertain [12], as a margin of 1.0 corresponds to the lowest reactor power consumption, but at the cost of a larger reactor design. Future designs may use a design margin of slightly higher than 1.0 to incorporate some flexibility in the electrode separation during operation.

It was shown that operating temperatures above the traditional paradigm of ∼1900 K are optimal for oxygen production levels above 500 kg/yr. Initially, it was unclear whether or not the benefits of a higher operating temperature would outweigh the drawbacks. Operating at a higher temperature allows the reactor to extract more oxygen per kilogram regolith and marginally decreases the total energy required for the chemical reactor (ΔH), while the drawbacks include increased heat loss and regolith heating power per kilogram regolith. The integrated model optimization results showed that operating temperatures closer to 2200 K result in a smaller holistic system mass.

The power breakdown shown in the top right of Figure 6 can also inform future designs. The bottom three sections in the graph (chemical and regolith heat up power) are somewhat immutable, but the radiative heat loss may be reduced via more complex insulation topologies. One elegant solution would be to place new regolith on the sides of the reactor prior to insertion, such that the heat that exits through the sides of the reactor goes directly into preheating the regolith. In this way, some portion of the "Radiative Heat Loss" power slice may go towards "Regolith Heating", thus reducing total power demand. Further power reduction may be achieved by recycling the heat generated by the oxygen liquefaction and storage system to preheat the regolith or supply some portion of the endothermic makeup requirement.

Future Work

There are a number of items that can be addressed in future work. The excavator system model currently does not produce an estimate of the energy consumed by the excavator, which would be an important addition to future models. Since the model's creation, newer excavation theory and models have also been developed [7, 26, 27], which can be integrated into the excavation model.

As mentioned in Section 2, the auger model is not yet parametrically sized to meet a given regolith insertion mass and time. Future work can dynamically size the radius and rotation rate of the auger to meet a specified insertion time that is compatible with the reactor model. This subsystem coupling would better inform an optimal reactor fill time and batch time.

One function that was not modeled in this work was the extraction of molten metals from the Molten Regolith Electrolysis reactor. Although a molten metal withdrawal system has been developed [19], the mass of the system and the interface between the withdrawal system and the reactor are uncertain. Future work can investigate incorporating a molten metal withdrawal model into the ISRU system model. By incorporating a withdrawal system model, future work will also examine the impact of MRE operating temperature with respect to metal and silicon product availability and production rate.

Future design iterations can also focus on including a spare parts analysis to more accurately determine the holistic mass of a less-than-ideal ISRU system.

ACKNOWLEDGMENTS

The authors would also like to thank Diane Linne, Juan Agui, Chris Gallo, and Greg Galloway for providing some of the subsystem models for the lunar ISRU system. We also thank Jesus Dominguez for his guidance on the theory behind the YSZ separator model and for providing some of the subsystem models. The authors thank Ariane Chepko for her advice concerning ISRU system model integration and Laurent Sibille for his guidance on the system-level considerations of Molten Regolith Electrolysis. This work was supported by a NASA Space Technology Research Fellowship (NASA Grant #NNX13AL76H).

REFERENCES

[1] L. A. Taylor and W. D. Carrier III, "Oxygen production on the moon: An overview and evaluation," *Resources of near earth space*, p. 69, 1993. 1

[2] B. Sherwood and G. R. Woodcock, "Cost and benefits of lunar oxygen: Economics, engineering, and operations," 1993. 1

[3] V. Badescu, *Moon: Prospective Energy and Material Resources*. Springer, 2012. 1

[4] D. L. Linne, "Employing isru models to improve hardware design," in *Proc., 48th AIAA Aerospace Sciences Meeting Including the New Horizons Forum and Aerospace Exposition*, 2010. 1

[5] E. Christiansen, C. H. Simonds, and K. Fairchild, "Conceptual design of a lunar oxygen pilot plant," *LPI Contributions*, vol. 652, p. 52, 1988. 1

[6] B. Altenberg, "Processing lunar in-situ resources," *Technical Research and Development Project Job*, no. 90634-002, 1990. 1

[7] G. B. Sanders and W. E. Larson, "Progress made in lunar in situ resource utilization under nasas exploration technology and development program," *Journal of Aerospace Engineering*, vol. 26, no. 1, pp. 5–17, 2012. 1, 10

[8] C. J. Steffen, J. E. Freeh, D. L. Linne, E. W. Faykus, C. A. Gallo, and R. D. Green, "System modeling of lunar oxygen production: Mass and power requirements," in *Proceedings of Space Nuclear Conference 2007*, 2007. 1

[9] A. Chepko, "Technology selection and architecture optimization of in-situ resource utilization systems," Ph.D. dissertation, Massachusetts Institute of Technology, 2009. 1, 2

[10] U. Hegde, R. Balasubramaniam, and S. Gokoglu, "Heating-rate-coupled model for hydrogen reduction of," *AIAA Proceedings*, 2010. 1

[11] R. Balasubramaniam, S. Gokoglu, and U. Hegde, "The reduction of lunar regolith by carbothermal processing using methane," *International Journal of Mineral Processing*, vol. 96, no. 1, pp. 54–61, 2010. 1

[12] S. S. Schreiner, L. Sibille, J. A. Dominguez, and A. H. Sirk, "A molten regolith electrolysis model for lunar in-situ resource utilization," *AIAA SciTech 2015: 8th Symposium on Space Resource Utilization*, 2015. 1, 2, 3, 5, 8, 9

[13] A. H. Sirk, D. R. Sadoway, and L. Sibille, "Direct electrolysis of molten lunar regolith for the production of oxygen and metals on the moon," *ECS Transactions*, vol. 28, no. 6, pp. 367–373, 2010. 1, 2

[14] P. Curreri, E. Ethridge, S. Hudson, T. Miller, R. Grugel, S. Sen, and D. Sadoway, "Process demonstration for lunar in situ resource utilizationmolten oxide electrolysis," *NASA Marshall Space Flight Center. MSFC Independent Research and Development Project*, no. 5-81, 2006. 1

[15] A. Colaprete, P. Schultz, J. Heldmann, D. Wooden, M. Shirley, K. Ennico, B. Hermalyn, W. Marshall, A. Ricco, R. C. Elphic *et al.*, "Detection of water in the lcross ejecta plume," *Science*, vol. 330, no. 6003, pp. 463–468, 2010. 1, 2

[16] D. Andrews, A. Colaprete, J. Quinn, D. Chavers, and M. Picard, "Introducing the resource prospector (rp) mission," in *AIAA Space 2014 Conference*, 2014. 2

[17] A. Chepko, O. de Weck, D. Linne, E. Santiago-Maldonado, and W. Crossley, "Architecture modeling of in-situ oxygen production and its impacts on lunar campaigns," in *AIAA SPACE 2008 Conference & Exposition*, 2008. 2

[18] L. Sibille, D. Sadoway, P. Tripathy, E. Standish, A. Sirk, O. Melendez, and D. Stefanescu, "Performance testing of molten regolith electrolysis with transfer of molten material for the production of oxygen and metals on the moon," *AIAA: 3rd Symposium on Space Resource Utilization*, 2010. 2

[19] L. Sibille and J. A. Dominguez, "Joule-heated molten regolith electrolysis reactor concepts for oxygen and metals production on the moon and mars," *50th AIAA Aerospace Sciences Meeting including the New Horizons Forum and Aerospace Exposition*, 2012. 2, 10

[20] D. A. O'Handley, E. E. Rice, and R. J. Gustafson, "Isru support for a self-sustaining lunar colony (sslc)," *39th AIAA Aerospace Sciences Meeting and Exhibit*, January 2001. 3

[21] S. Heiroth, T. Lippert, A. Wokaun *et al.*, "Microstructure and electrical conductivity of ysz thin films pre-

pared by pulsed laser deposition," *Applied Physics A*, vol. 93, no. 3, pp. 639–643, 2008. 3

[22] J. Wang, Z. Lü, X. Huang, K. Chen, N. Ai, J. Hu, and W. Su, "Ysz films fabricated by a spin smoothing technique and its application in solid oxide fuel cell," *Journal of power sources*, vol. 163, no. 2, pp. 957–959, 2007. 4

[23] C. A. Gallo, R. A. Wilkinson, R. P. Mueller, J. Schuler, and A. Nick, "Comparison of isru excavation system model blade force methodology and experimental results," *American Institute of Aeronautics and Astronautics (AIAA)*, 2009. 4

[24] R. Lindemann and C. Voorhees, "Mars exploration rover mobility assembly design, test and performance," in *2005 IEEE International Conference on Systems, Man and Cybernetics*, vol. 1, Oct 2005, pp. 450–455 Vol. 1. 4

[25] A. J. Hanford, "Advanced life support baseline values and assumptions document," 2006. 5

[26] K. Zacny, R. Mueller, G. Galloway, J. Craft, G. Mungas, M. Hedlund, and P. Fink, "Novel approaches to drilling and excavation on the moon," in *AIAA SPACE Conference & Exposition*, 2009, pp. 6431–6443. 10

[27] K. Zacny, P. Chu, G. Paulsen, J. Spring, M. Hedlund, J. Craft, P. van Susante, R. Mueller, G. Galloway, and J. Mantovani10, "Parametric optimization and prediction software for excavation and prospecting tasks," 2013. 10

BIOGRAPHY

Samuel S. Schreiner *is a NASA Space Technology Research Fellow in the Department of Aeronautics and Astronautics at MIT and is pursuing a Masters in Aerospace Engineering with a focus on space systems engineering. He received a Bachelors of Aerospace Engineering and Mechanics from the University of Minnesota (summa cum laude) in 2013. He conducts research at MIT modeling In-Situ Resource Utilization technology to produce oxygen and other resources from planetary regolith.*

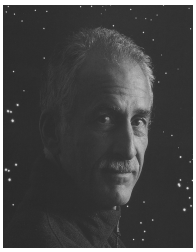

Dr. Jeffrey Hoffman *is a professor in MITs Aeronautics and Astronautics Department. He received a BA in Astronomy (summa cum laude) from Amherst College (1966); a PhD in Astrophysics from Harvard University (1971); and an MSc in Materials Science from Rice University (1988). As a NASA astronaut (1978-1997) Dr. Hoffman made five space flights, becoming the first astronaut to log 1000 hours of flight time aboard the Space Shuttle. His primary research interests are in improving the technology of space suits and designing innovative space systems for human and robotic space exploration. Dr. Hoffman is director of the Massachusetts Space Grant Consortium. In 2007, Dr. Hoffman was elected to the US Astronaut Hall of Fame.*

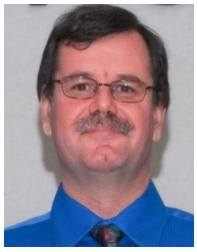

Gerald Sanders *received his B.S. degree in Aerospace Engineering from the University of Cincinnati in 1987. He currently works in the Propulsion and Power Division at the NASA Johnson Space Center, in Houston Texas. Mr. Sanders has worked in the area of In-Situ Resource Utilization (ISRU) for over 19 years, and currently serves as ISRU Chief Engineer.*

Kristopher A. Lee *received his B.S. degree in Mechanical Engineering in 1995 and a M.S. degree in Electrical Engineering from Texas A&M Universtiy in 1998. He currently works in the Propulsion and Power Division at the NASA Johnson Space Center where he designs and develops embedded control and monitoring applications for hardware in support of In-Situ Resource Utilization research and development.*